

Structure of Isolated and Solvated Peroxyl Radicals

P. APLINCOURT,^{1,2} M. F. RUIZ-LÓPEZ,¹ X. ASSFELD,¹ F. BOHR²

¹Laboratoire de Chimie théorique, UMR CNRS-UHP No. 7565 (Institut Nancéen de chimie Moléculaire), Université Henri Poincaré, Nancy I, B.P. 239, 54506 Vandoeuvre-lès-Nancy Cedex, France

²Laboratoire de Chimie Physique, GSMA, UPRES-A 6089, Université de Reims, Faculté des Sciences, Moulin de la Housse, B.P. 1039, 51687 Reims Cedex 2, France

Received 27 October 1998; accepted 25 February 1999

ABSTRACT: We have investigated the structure of HO₂ and a series of alkyl peroxy radicals ROO using a variety of quantum mechanical methods. We first compute the geometries, vibrational frequencies, electronic charge distributions, and spin densities for the series of radicals considered in the gas phase. Significant differences with respect to previous calculations have been pointed out in a few cases. In particular, we show the fundamental importance of electronic correlation when computing net atomic charges and spin densities, which have generally been estimated in the literature by means of Hartree–Fock SCF electronic densities. Solvation effects on the geometry and electronic structure have been estimated by carrying out self-consistent reaction field computations in a polarizable continuum environment with relative dielectric permittivity equal to that of liquid water. Large electronic polarization is predicted in such conditions. This may be important in order to understand reactive properties of the radicals in different media. © 1999 John Wiley & Sons, Inc. *J Comput Chem* 20: 1039–1048, 1999

Keywords: peroxy radicals; atmospheric chemistry; theoretical calculations; solvation effects; spin density

Introduction

Peroxy radicals are important intermediates in a variety of chemical and biochemical reactions. They play a central role in atmospheric

Correspondence to: M. F. Ruiz-López; e-mail: Manuel.Ruiz@lctn.u-nancy.fr

chemistry,¹ especially in reactions connected to ozone formation or depletion. For instance, the increase of tropospheric ozone concentration in the vicinity of big cities is due to oxidation reactions of volatile organic compounds by the OH radical. This yields peroxy radicals ROO, which in turn, oxidize NO to yield NO₂, modify the equilibrium ratio of the NO/NO₂ couple and favor ozone formation. In the stratosphere, the hydroperoxy

radical HO_2 is an essential species that participates to the catalytic cycle of ozone depletion. Ionic dissociation of HO_2 is also a key process in the decomposition of ozone in the presence of cloud droplets. Peroxyl radicals are also found in combustion processes,² polymer degradation,³ as well as in biological reactions^{4,5} such as the autooxidation of cholesterol and oleate esters.

The study of the electronic structure and reactive properties of peroxyl radicals is, therefore, of wide interest, and naturally it has attracted much experimental^{6–21} and theoretical^{22–31} attention. The geometry and vibrational frequencies of the smallest species have been determined.^{6–13} Electron Spin Resonance measurements have been reported.^{14,15} Dissociation energies into R and O_2 for several radicals are also available.^{16–18} Theoretical computations have been mainly focused on the geometry and charge distribution of the radicals,^{22–26} although some work has also been devoted to the reactivity,^{27–31} excited states,³² and hyperfine couplings.^{21,33} Most of these theoretical studies have been carried out at the *ab initio* level using unrestricted Hartree–Fock (UHF) or different correlated methods, essentially through the second-order Moller–Plesset theory (MP2).^{22,24,26,30} Semiempirical calculations have been reported also,²² but such an approach appears to give poor results. Recently, the Density Functional Theory (DFT) has been applied to study some peroxyl radicals with encouraging results,^{27,28,31,34} but work is still necessary to check the aptness of this method to correctly describe the properties of such radicals.

In this article, we have carried out further theoretical computations at different levels for a series of peroxyl radicals trying to clarify the following points: (1) how the electronic charge and spin density are distributed, particularly in O atoms; (2) how solvation modifies the structure of the species; and (3) what is the influence of the computational level on results. Some discussion on these points has already been considered in the literature, but as we show below, our results significantly modify previous conclusions. The effect of hydration on HO_2 reactivity has already been investigated³⁵ using small clusters to model interactions in water droplets. Our purpose here is to estimate the role of aqueous solvent on peroxy radicals, which, being polar species, are expected to undergo substantial perturbations arising from long-range electrostatic interactions.

Computations

We studied a series of RO_2 radicals, with $\text{R} = \text{H}$, CH_3 , CH_3CH_2 , $\text{CH}_3\text{CH}_2\text{CH}_2$, CHC , CH_2CH , and CH_3CH_2 . Computations are carried at the QCISD and DFT levels for the smallest species using the 6–311++G(d,p) basis set. DFT calculations are done using the gradient-corrected functional BLYP,^{36,38} as well as the hybrid B3LYP^{37,38} functional. Because the agreement between QCISD and DFT results for the radicals with $\text{R} = \text{H}$, CH_3 is quite satisfactory, and both methods reproduce the available experimental quantities well, for the other systems, only DFT computations (which are much less time consuming) have been performed. These computational levels could not be suitable to investigate other properties, such as bond dissociation energies, which may require the use of more accurate methods. Nevertheless, they are adequate to the purpose of this article, which is basically the qualitative study of the electronic distribution of peroxyl radicals as a function of alkyl chain and molecular environment.

To compare with other data in the literature (in particular, for electron and spin densities), we have also carried out UHF and MP2 calculations. Expectation values of S^2 found in this study are below 0.763, except for the ethenyl radical (0.804 at the UHF level), indicating a small spin contamination. Harmonic vibrational frequencies are determined analytically for all methods. Net atomic charges are computed with the CHELPG³⁹ and GRID⁴⁰ algorithms. For comparison, a Mulliken population analysis is also performed. Solvent effects are evaluated using the SCRFPAC program,⁴¹ in which the solvent (water) is modeled by a polarizable dielectric continuum⁴² with dielectric constant $\epsilon_0 = 80$. However, for comparison purposes, we also include some computations carried out using a typical dielectric constant for a nonpolar solvent ($\epsilon_0 = 2$). Moreover, results obtained using discrete and mixed discrete-continuum models are presented and discussed. The computations in that case have been done at the B3LYP/6–31+G** level. All the calculations have been carried out with the Gaussian94 program.⁴³

Basically, the electrostatic solvent effect due to the continuum medium is computed as follows. The solute is assumed to be placed in a cavity adapted to the molecular shape and embedded in a dielectric medium, which is polarized by the

solute's charge distribution. The electric field created by the polarized dielectric is then computed and included in the solute's Hamiltonian, so that polarization effects are considered explicitly and evaluated by a self-consistent technique. The main difference of this SCRf method with respect to other implementations of the continuum approach⁴⁴ lies in the method to compute the solvent reaction field. In Nancy's group approach⁴² the reaction field is obtained using a multipolar development of the electrostatic potential. The advantage of this technique is that the main quantities (molecular multipoles, reaction field factors) are calculated as straightforward, using analytical formulae that may easily be derived, allowing for very fast geometry optimization.

Results

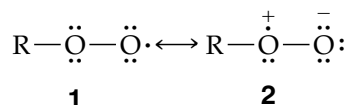
STRUCTURE OF HO₂

Let us first discuss the results obtained for the simplest species HO₂ in the gas phase. The computed geometry is given in Figure 1; vibrational frequencies and dipole moment are summarized in Table I; spin densities and net atomic charges are given in Tables II and III, respectively. *Ab initio* calculations at the UHF and MP2 levels compare well with previous results at the same level.²² As usual, at the UHF level, bond lengths are underestimated. The introduction of electronic correlation via Møller–Plesset perturbation theory (MP2) substantially reduces the error in such quantities. An MP4 calculation⁴ gives results a little closer to the experiment ($d_{\text{OO}} = 1.324 \text{ \AA}$, $d_{\text{OH}} = 0.977 \text{ \AA}$). QCISD results are quite close to the experiment. At the DFT level, the BLYP functional overestimates the bond distances a little, but the hybrid B3LYP functional yields satisfactory the results. In all cases, the bond angle is predicted quite reasonably. The dipole moment is always a little overestimated, especially by DFT methods. The relatively good agreement between the experimental and UHF dipole moments is fortuitous, as we discuss below. Harmonic vibrational frequencies at the DFT level are predicted within 5%, whereas errors for either UHF or MP2 are much larger.

A noticeable discrepancy between UHF and other methods concerns spin densities, as shown in Table II. UHF spin density on the outer O atom is substantially overestimated with respect to MP2, QCISD, or DFT calculations that agree to predict

values of about 0.7–0.8 and 0.2–0.3 for the spin density on outer and inner O atoms, respectively.

Because previous computations of net atomic charges for peroxy radicals were based on the Mulliken Population Analysis, we also include net Mulliken charges in Table III. One must note, in addition, that previous works have been based on Hartree–Fock electron densities (even for those calculations carried out at the MP2 level). The atomic charges in Table III display some interesting features. As in the case of spin densities, taking into account corrections due to electron correlation interactions is fundamental. Roughly, all the correlated levels (*ab initio* or DFT) lead to comparable results differing from UHF in that the negative charge on O atoms is substantially shifted towards the outer one. Taken the Mulliken charges, one may note that for UHF the inner oxygen atom has a large negative charge, whereas the charge on the outer O is very small. This result has been obtained before, and has led to the conclusion that the importance of structure 2 (see Scheme) in explaining the high polarity of peroxy radicals is minor.²⁴ Nevertheless, we see here that when electron densities from correlated methods are used, both oxygen atoms carry a significant negative charge. CHELPG and GRID charges are substantially different from Mulliken values, but corroborate that the weight of the formal structure 2 increases when electronic correlation is considered. One may expect that by changing H by an alkyl group, structure 2 will be further stabilized due to inductive effects, so that the charge on the outer O atom becomes larger than that on the inner one. This is indeed found by our calculations, as shown below.



SUBSTITUENT EFFECTS ON RO₂

Geometry parameters for the other radicals studied are given in Figure 1. Dipole moments and spin densities are gathered in Table IV. Only the most stable conformations are considered (see Fig. 1). Note that the agreement between DFT and QCISD calculations, although no perfect, is reasonably good.

It is interesting to analyze how the properties vary along the series R = CH₃, CH₃CH₂, and CH₃CH₂CH₂ (series I) and R = CH₃CH₂, CH₂CH

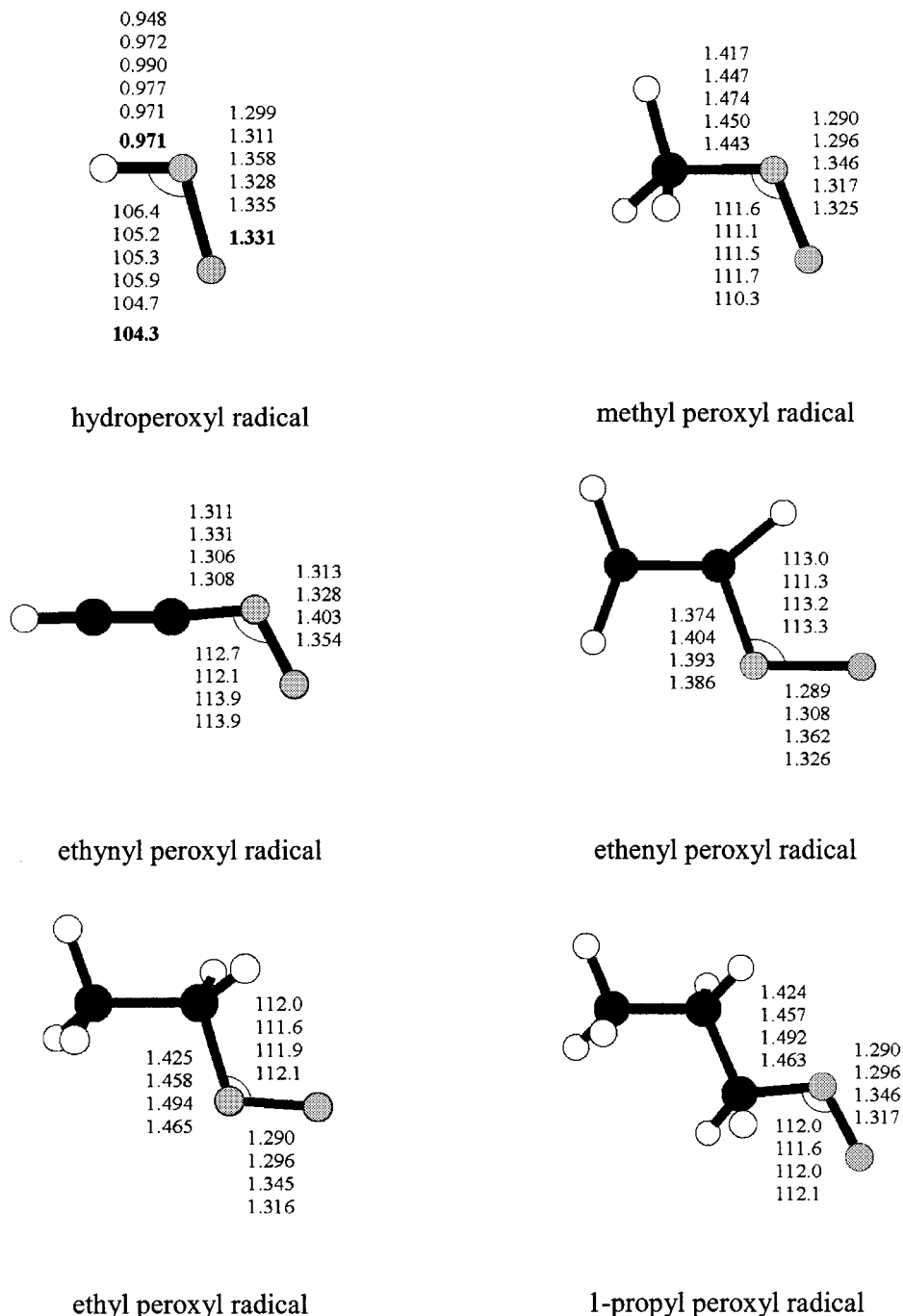


FIGURE 1. Most stable conformations of the peroxy radicals studied in this work.

and CHC (series II). Similar remarks apply for all methods, although the absolute value of a given quantity may be quite dependent on the theoretical level, as for HO_2 .

The OO length in series I changes very little, the bond being shorter by about 0.1 Å than in the parent radical HO_2 . In the same series, the CO bond increases a little ($1\text{--}2 \times 10^{-2}$ Å) in going from

$\text{R} = \text{CH}_3$ to $\text{R} = \text{CH}_3\text{CH}_2$, but is practically unchanged by further enlargement of the alkyl chain. The dipole moment increases along the series and is significantly larger than in HO_2 . The spin densities are not quite sensitive to the size of the alkyl group, but one may note that the ratio outer/inner oxygen atom diminishes with respect to HO_2 . For the correlated methods, this ratio is not far from 2,

TABLE I.
Vibrational Frequencies (cm^{-1}) and Dipole Moment (debye) of the HO_2 Radical in the Gas Phase.

	ν_1	ν_2	ν_3	μ
UHF	1269	1605	4059	2.122
MP2	1232	1451	3703	2.299
BLYP	1051	1351	3411	2.410
B3LYP	1157	1423	3593	2.381
QCISD				2.279
Exp.	1098 ^a	1392 ^b	3436 ^c	2.090

^a See ref. 13.^b See ref. 12.^c See ref. 11.

which is compatible with ESR experimental information¹⁴ and other DFT calculations³³ that suggest that spin density on the terminal oxygen atom is approximately twice the value on the inner one. Other works have predicted higher ratios²⁴ because of the use of Hartree–Fock densities (see also our UHF results).

In series II, the degree of insaturation of the alkyl group changes and this plays a significant role on the radical structure. The OO bond lengths increase along the series (except in the case of the UHF value from $\text{CH}_3\text{CH}_2\text{OO}$ to CH_2CHOO). Conversely, the CO bond is substantially shortened. The spin densities change is more marked than in the first series, but there is not a uniform agreement between the methods. For instance, MP2 predicts a spin-density increase for the outer oxygen from $\text{CH}_3\text{CH}_2\text{OO}$ to CH_2CHOO , whereas UHF, BLYP, and B3LYP predict a decrease.

The analysis of net atomic charges is made from data in Table V for the CH_3OO radical. Only this radical is considered for simpleness because the results for the other species lead to similar conclusions. As found for the simple HO_2 radical, the

TABLE II.
Spin Densities of the HO_2 Radical in the Gas Phase.

	O _{outer}	O _{inner}	H
UHF	0.908	0.105	−0.013
MP2	0.742	0.273	−0.015
BLYP	0.714	0.296	−0.010
B3LYP	0.740	0.270	−0.010
QCISD	0.783	0.229	−0.012

role of correlation is quite important, independently of the method used to evaluate the atomic charge. Using the results of correlated methods we predict that the outer oxygen atom carries a negative charge that is much larger than the one carried by the inner O atom, contrary to UHF predictions here or in previous works.²⁴ Obviously, the absolute charges depend on the population analysis approach, but qualitatively the trends are the same.

SOLVENT EFFECTS IN AQUEOUS SOLUTION

To evaluate the effect of aqueous solvation on the structure of peroxy radicals we have studied the simplest species HO_2 and CH_3O_2 in aqueous solution using a polarizable continuum model for the solvent. We use a general cavity shape and a multipole expansion of the solvation energy including terms up to the sixth order. The dielectric constant of the medium is 80.

Tables VI and VII summarize the results for the geometry, spin densities, and atomic charges for HO_2 , whereas Tables VIII and IX contain the same information for CH_3O_2 . Solvent effects of the internal geometrical parameters are not very large. In general, the calculations predict a small decrease of the OO bond (except for BLYP in CH_3O_2) and a small increase of OH or OC bonds. The main effects appear for the electronic charge distribu-

TABLE III.
Net Atomic Charge of the HO_2 Radical in the Gas Phase.

	Mulliken			CHelpG			GRID		
	O _{outer}	O _{inner}	H	O _{outer}	O _{inner}	H	O _{outer}	O _{inner}	H
UHF	−0.038	−0.229	0.267	−0.069	−0.355	0.424	−0.069	−0.364	0.413
MP2	−0.122	−0.138	0.260	−0.135	−0.271	0.406	−0.134	−0.280	0.414
BLYP	−0.163	−0.100	0.263	−0.165	−0.228	0.393	−0.163	−0.236	0.399
B3LYP	−0.146	−0.121	0.267	−0.152	−0.252	0.404	−0.151	−0.261	0.412
QCISD	−0.125	−0.128	0.253	−0.136	−0.264	0.400			

TABLE IV.
Dipole Moments (debye) and Spin Densities for Alkyl-Substituted Peroxyl Radicals.

	R =	CH ₃	CH ₃ CH ₂	CH ₃ CH ₂ CH ₂	CHC	CH ₂ CH
μ	UHF	2.548	2.670	2.753	1.389	2.088
	MP2	2.894	3.089	3.207	1.772	2.488
	BLYP	3.043	3.351	3.502	2.801	3.254
	B3LYP	2.980	3.235	3.368	2.373	2.982
	QCISD	2.812				
Spin density O _{inner}	UHF	0.120	0.118	0.122	0.081	0.133
	MP2	0.321	0.321	0.323	0.225	0.269
	BLYP	0.323	0.327	0.329	0.216	0.260
	B3LYP	0.299	0.302	0.304	0.218	0.263
	QCISD	0.257				
Spin density O _{outer}	UHF	0.890	0.893	0.890	0.926	0.877
	MP2	0.683	0.686	0.685	0.766	0.785
	BLYP	0.663	0.662	0.661	0.638	0.614
	B3LYP	0.693	0.692	0.692	0.698	0.660
	QCISD	0.744				

tion. According to formal structures 1 and 2 above, one could expect that the main polar environment effect would essentially favor structure 2, leading to a net increase of the radical polarity. Our results confirm that there is a strong increase of the dipole moment in solution, demonstrating that these systems are quite polarizable. However, the previous interpretation is too simple. Indeed, there is a net electron density transfer from the alkyl group to the O₂ fragment so that total negative charge on the latter always increases. The excess of charge is delocalized more or less uniformly (depending on system and method) on the two O atoms. Note also that the spin density on the outer oxygen decreases moderately through solvent effects.

The energetics of the solvation process is detailed on Table X. The values given correspond to the electrostatic + polarization solvation term (i.e.,

we do not include cavitation and dispersion contributions). Although small variations are found among the different methods, the solvation energy for the smallest radical HO₂ is approximately 1 kcal/mol larger than that for CH₃O₂. The detailed analysis of the multipole contributions shows that

TABLE VI.
Geometry (Å, Degrees) and Dipole Moment (debye) of the HO₂ Radical in Aqueous Solution.

	d _∞	d _{OH}	α	μ
UHF	1.296	0.950	106.8	2.398
MP2	1.307	0.974	106.1	2.625
BLYP	1.355	0.991	105.8	2.851
B3LYP	1.325	0.979	106.4	2.786

TABLE V.
Net Atomic Charge of the CH₃O₂ Radical in the Gas Phase.

	Mulliken			CHelpG			GRID		
	O _{outer}	O _{inner}	R	O _{outer}	O _{inner}	R	O _{outer}	O _{inner}	R
UHF	-0.030	-0.145	0.175	-0.106	-0.179	0.285	-0.144	-0.168	0.312
MP2	-0.139	-0.027	0.166	-0.187	-0.095	0.282	-0.221	-0.102	0.323
BLYP	-0.175	-0.017	0.192	-0.208	-0.073	0.281	-0.241	-0.084	0.325
B3LYP	-0.158	-0.030	0.188	-0.198	-0.084	0.272	-0.233	-0.092	0.325
QCISD	-0.128	-0.037	0.165	-0.174	-0.106	0.280			

TABLE VII.
Spin Densities and Net Atomic Charges of the HO₂ Radical in Aqueous Solution.

	Spin Densities			Net Atomic Charges					
	O _{outer}	O _{inner}	H						
UHF	0.899	0.113	−0.012						
MP2	0.725	0.290	−0.015						
BLYP	0.691	0.319	−0.010						
B3LYP	0.718	0.292	−0.010						
	Mulliken			CHelpG			GRID		
	O _{outer}	O _{inner}	H	O _{outer}	O _{inner}	H	O _{outer}	O _{inner}	H
UHF	−0.052	−0.253	0.305	−0.086	−0.383	0.469	−0.086	−0.393	0.479
MP2	−0.140	−0.161	0.301	−0.157	−0.300	0.457	−0.135	−0.281	0.416
BLYP	−0.201	−0.107	0.308	−0.207	−0.240	0.447	−0.207	−0.249	0.456
B3LYP	−0.181	−0.130	0.311	−0.191	−0.266	0.457	−0.190	−0.276	0.466

TABLE VIII.
Geometry (Å, Degrees) and Dipole Moment (debye) of the CH₃O₂ Radical in Aqueous Solution.

	d _∞	d _{OC}	α _{OOC}	μ
UHF	1.288	1.425	111.9	2.989
MP2	1.293	1.454	111.5	3.416
BLYP	1.346	1.479	112.0	3.760
B3LYP	1.316	1.456	112.1	3.625

TABLE X.
Solvation Energies (in kcal / mol) for HO₂ and CH₃O₂ Radicals.

	HO ₂	CH ₃ O ₂
UHF	−3.7	−2.6
MP2	−3.9	−3.0
BLYP	−4.3	−3.5
B3LYP	−4.2	−3.4

TABLE IX.
Spin Densities and Net Atomic Charges of the CH₃O₂ Radical in Aqueous Solution.

	Spin Densities			Net Atomic Charges					
	O _{outer}	O _{inner}	R						
UHF	0.879	0.131	−0.010						
MP2	0.658	0.347	−0.005						
BLYP	0.637	0.346	−0.015						
B3LYP	0.667	0.324	−0.009						
	Mulliken			CHelpG			GRID		
	O _{outer}	O _{inner}	R	O _{outer}	O _{inner}	R	O _{outer}	O _{inner}	R
UHF	−0.045	−0.168	0.213	−0.128	−0.200	0.328	−0.167	−0.199	0.366
MP2	−0.163	−0.045	0.208	−0.219	−0.110	0.329	−0.256	−0.128	0.384
BLYP	−0.219	−0.024	0.243	−0.260	−0.078	0.338	−0.327	−0.183	0.510
B3LYP	−0.197	−0.037	0.234	−0.246	−0.087	0.333	−0.285	−0.106	0.391

the largest one comes from the dipole term, as expected. In the case of HO_2 , the dipole moment contribution reaches 80% of the total electrostatic solvation energy, whereas for CH_3O_2 it represents 90%. The quadrupole moment contribution accounts in both cases for almost the rest of the electrostatic solvation energy. It must be noted that although CH_3O_2 has a larger dipole moment (compared to HO_2), its solvation energy is lower. This is due to the augmentation of the molecular volume, which predominates over the dipole moment increase. The polarization energy, which represents the difference in electrostatic solvation energy for the solute with its gas-phase charge distribution and that for the fully relaxed solute, is 0.5 and 0.6 kcal/mol for HO_2 and CH_3O_2 , respectively, which represent around 12 and 18% of the corresponding total electrostatic terms.

The previous results may be compared to those obtained in other environments. Such a comparison is made in Table XI. On one hand, we have calculated the solvent effect on CH_3O_2 in a medium with small dielectric constant ($\epsilon_o = 2$). It should be remembered that the reaction field (i.e., the potential generated by the polarized solvent), and therefore the solvation energy, does not vary linearly with the dielectric constant. Roughly, in Onsager's model⁴⁵ the electric field inside the cavity is proportional to the quantity $2(\epsilon_o - 1)/(2\epsilon_o + 1)$. On the other hand, we have evaluated the effect due to specific interactions, i.e., hydrogen bonds. In the latter case, we have considered a complex formed by the solute with three water molecules, the complex being isolated or surrounded by a dielectric continuum with $\epsilon_o = 80$. The structure of the tri-hydrated complex, as optimized in the gas phase, is displayed in Figure 2. Note that the structure of the tri-hydrated complex is consistent with that reported for several hy-

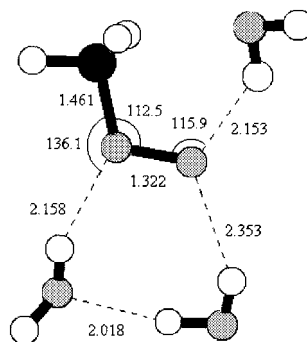


FIGURE 2. Optimized structure in the gas phase of the hydrated CH_3O_2 radical at the B3LYP / 6-31 + G** level.

drated complexes for HO_2 ³⁵ except that, in the present case, the hydrophobic methyl group, in contrast to the hydrophilic hydrogen in HO_2 , does not form hydrogen bonds with water molecules.

The role played by a medium of low dielectric constant is not very large, although it represents a nonnegligible part of the effect found in the polar medium, and of course, both go in the same direction. More interesting are the results obtained for the hydrogen bonds. First, one must remark that the total charge transfer from peroxy to water molecules is substantial but not quite dependent on the medium surrounding the complex. If one compares the charge distribution in the isolated complex and peroxy (lines 1 and 4), one notes that the charge transfer is made basically from the O_2 unit, the methyl group charge being practically unchanged by the presence of water molecules. In a polar medium (lines 3 and 5), the polarization effects predicted by the continuum and discrete-continuum models are comparable, the total electronic density transferred from the methyl group to O_2 being similar in both models, although the

TABLE XI.
Comparison of Net Atomic Charges (Computed with CHelpG) for the CH_3O_2 Radical in Different Environments Computed at the B3LYP / 6-31 + G** Level.

	O_{outer}	O_{inner}	Total O_2	CH_3	Δq^a
Gas	-0.196	-0.089	-0.285	0.285	
$\epsilon_o = 2$	-0.214	-0.091	-0.305	0.305	
$\epsilon_o = 80$	-0.242	-0.094	-0.336	0.336	
Isolated complex	-0.158	0.033	-0.125	0.283	-0.157
Solvated complex ($\epsilon_o = 80$)	-0.171	0.001	-0.170	0.325	-0.154

For simplicity, the calculations in solution have been done using the optimized geometries in vacuum for the peroxy radical and the peroxy-water complex.

^a Total charge transfer to water molecules.

redistribution of this density within the O₂ unit depends on the model used.

In summary, long-range electrostatic interactions and hydrogen bonds play both a substantial role on the charge distribution of RO₂ peroxy radicals in aqueous solution. The former are mainly responsible for internal charge transfer R → O₂, whereas the latter allows for intermolecular charge transfer RO₂ → H₂O.

Conclusions

Calculations at the UHF level are often in poor agreement with available experimental data for peroxy radicals. When correlation effects are accounted for at the MP2 level, the results are substantially improved, but some quantities are still inaccurate. Very little DFT calculations for this type of radicals have been reported in the literature, and our computations allow us to make a critical discussion on their suitability. Indeed, the BLYP or the B3LYP functionals are overall satisfactory, especially in the latter case, and reasonably conclusions may be reached with them. This is an interesting remark, because for large radicals, the employ of high level *ab initio*-correlated methods is not affordable. Note, however, that some quantities are difficult to obtain accurately (for instance, the dipole moment of HO₂) and require the use of sophisticated approaches such as QCISD. One of the most striking results obtained is that electron correlation corrections are essential to predict, even qualitatively, spin densities and atomic charges, which are very poor when UHF densities are used. In particular, we have shown that previous conclusions on oxygen atomic charges derived from the Hartree–Fock density are wrong. The outer oxygen atom charge is always substantial and larger than the inner oxygen atom one when alkyl derivatives are considered. Moreover, in aqueous solution, solvation effects modify a lot of the electronic distribution of the radicals, which are quite polarizable species, even if the geometry changes due to solvation are rather small. The polarization is not simply due to stabilization of the zwitterionic formal structure 2 by solvation, but mainly to a net electronic charge transfer from the alkyl group to the O₂ fragment. Despite the dipole moment increase along the RO₂ series (R = H, CH₃, CH₂CH₃, CH₂CH₂CH₃...), the electrostatic solvation energy may be lower as a consequence of the molecular volume augmentation, as found for

HO₂ and CH₃O₂. Hydrogen bonds with solvent molecules may also be important, because they allow to delocalize the electronic density on oxygen atoms.

References

1. Heiklen, J. *Atmospheric Chemistry*; Academic Press: New York, 1977; *The Chemistry of Free Radicals: Peroxyl Radicals*; Alfassi, Z. B., Ed.; John Wiley & Sons: New York, 1997.
2. Hucknall, K. J. *Chemistry of Hydrocarbon Combustions*; Chapman and Hall: New York, 1985.
3. Carlsson, D. J.; Dobbin, C. J. B.; Wiles, D. M. *Macromolecules* 1985, 18, 2092.
4. Schenck, G. O.; Neumuller, O. A.; Eisfeld, W. *J Liebigs Ann Chem* 1958, 618, 202.
5. Brill, W. E. *J Am Chem Soc* 1965, 87, 3286.
6. Beers, Y.; Howard, C. J. *J Chem Phys* 1976, 64, 1541.
7. Lubic, K. G.; Amano, T.; Uehara, H.; Kawaguchi, K.; Hirota, E. *J Chem Phys* 1984, 81, 4826.
8. Barnes, C. E.; Brown, J. M.; Radford, H. E. *J Mol Spectrosc* 1980, 84, 179.
9. Ase, P.; Bock, W.; Snelson, A. *J Phys Chem* 1986, 90, 2099.
10. Chettur, G.; Snelson, A. *J Phys Chem* 1987, 91, 3483.
11. Yamada, C.; Endo, Y.; Hirota, E. *J Chem Phys* 1983, 78, 4379.
12. Nagai, K.; Endo, Y.; Hirota, E. *J Mol Spectrosc* 1981, 89, 520.
13. Johns, J. W. C.; McKellar, A. R. W.; Riggan, M. *J Chem Phys* 1978, 68, 3957.
14. Adamic, K.; Ingold, K. U.; Morton, J. R. *J Am Chem Soc* 1970, 92, 922.
15. Adrian, F. J.; Cochran, E. L.; Bowers, V. A. *J Chem Phys* 1967, 47, 5441.
16. Benson, S. W. *J Am Chem Soc* 1975, 87, 972.
17. Slagle, I. R.; Feng, Q.; Gutman, D. *J Phys Chem* 1984, 88, 3648.
18. Knyazev, V. D.; Slagle, I. R. *J Phys Chem* 1998, 102, 1770.
19. Horie, O.; Crowley, J. N.; Moortgat, G. K. *J Phys Chem* 1990, 94, 8198.
20. Hayman, G. D.; Battin-Leclerc, F. *J Chem Soc Faraday Trans* 1995, 91, 1313.
21. Nelander, B. *J Phys Chem* 1997, 101, 9092.
22. Besler, B. H.; Sevilla, M. D.; MacNeille, P. *J Phys Chem* 1986, 90, 6446.
23. Bair, R. A.; Goddard, W. A., III. *J Am Chem Soc* 1982, 104, 2719.
24. Boyd, S. L.; Boyd, R. J.; Barclay, L. R. C. *J Am Chem Soc* 1990, 112, 5724.
25. Quelch, G. E.; Gallo, M. M.; Schaefer, H. F., III. *J Am Chem Soc* 1992, 114, 8239.
26. Garcia, I.; Uc, V.; Ruiz, M. E.; Smeyers, Y. G.; Vivier Bunge, A. *J Mol Struct (THEOCHEM)* 1995, 340, 149.
27. Jursic, B. S. *J Phys Chem* 1997, 101, 2345.
28. Henon, E.; Bohr, F.; Chakir, A.; Brion, J. *Chem Phys Lett* 1997, 264, 557.

29. Shen, D.; Moise, A.; Pritchard, H. O. *J Chem Soc Faraday Trans* 1995, 91, 1425.
30. Boyd, S. L.; Boyd, R. J.; Shi, Z.; Barclay, L. R. C.; Porter, N. A. *J Am Chem Soc* 1993, 115, 687.
31. Green, W. H. *Int J Quantum Chem* 1994, 52, 837.
32. Jafri, J. A.; Phillips, D. H. *J Am Chem Soc* 1990, 112, 2586.
33. Wetmore, S. D.; Boyd, R. J.; Erikson, L. A. *J Chem Phys* 1997, 106, 7738.
34. Jungkamp, T. P. W.; Smith, J. N.; Seinfeld, J. H. *J Phys Chem* 1997, 101, 4392.
35. Pérez del Valle, C.; Valdemoro, C.; Novoa, J. J. *J Mol Struct (THEOCHEM)* 1996, 371, 143.
36. Becke, A. D. *Phys Rev A* 1988, 38, 3098.
37. Becke, A. D. *J Chem Phys* 1993, 98, 5648.
38. Lee, C.; Yang, W.; Parr, R. G. *Phys Rev B* 1988, 37, 785.
39. Breneman, C. M.; Wiberg, K. B. *J Comput Chem* 1990, 11, 361.
40. Chipot, C.; Ángyán, J. G. GRID Version 3.1: Point Multipoles Derived From Molecular Electrostatic Properties; QCPE No. 655, 1994.
41. Rinaldi, D.; Pappalardo, R. R. SCRFPAC; QCPE, Indiana University, Bloomington, IN, 1992; program number 622, Adapted version for Gaussian 94 by D. Rinaldi.
42. Rivail, J. L.; Rinaldi, D. In *Computational Chemistry. Reviews of Current Trends*; Leszczynski, J., Ed.; World Scientific Pub.: Singapore, 1996, p. 139.
43. Frisch, M. J.; Trucks, G. W.; Schlegel, H. B.; Gill, P. M. W.; Johnson, B. G.; Robb, M. A.; Cheeseman, J. R.; Keith, T.; Petersson, G. A.; Montgomery, J. A.; Raghavachari, K.; Al-Laham, M. A.; Zakrzewski, V. G.; Ortiz, J. V.; Foresman, J. B.; Peng, C. Y.; Ayala, P. Y.; Chen, W.; Wong, M. W.; Andres, J. L.; Replogle, E. S.; Gomperts, R.; Martin, R. L.; Fox, D. J.; Binkley, J. S.; Defrees, D. J.; Baker, J.; Stewart, J. P.; Head-Gordon, M.; Gonzalez, C.; Pople, J. A. GAUSSIAN 94, Revision B.3; Gaussian Inc.: Pittsburgh, PA, 1995.
44. See the following reviews: Tomasi, J.; Persico, M. *Chem Rev* 1994, 94, 2027; Cramer, C. J.; Truhlar, D. G. *Reviews in Computational Chemistry*; Lipkowitz, K. B.; Boyd, D. B., Eds.; VCH Publishers, Inc.: New York, 1995, p. 1, vol. VI.
45. Onsager, L. *J Am Chem Soc* 1936, 58, 1486.